



ARTICLE

Exploring the phenotypic spectrum and osteopenia mechanisms in Yunis-Varón syndrome



Éliane Beauregard-Lacroix¹, Alexandra Scott¹, Thi Tuyet Mai Nguyen², Klaas J. Wierenga³, Gabriela Purcarin⁴, Anne B. Karstensen^{5,6}, Daniel R. Carvalho⁷, Jean-Luc Alessandri⁸, Frédérique Payet⁹, Katta M. Girisha^{10,11}, Mathieu Ferron^{12,13}, Philippe M. Campeau^{1,2,*} 

ARTICLE INFO

Article history:

Received 11 August 2023

Received in revised form

7 March 2024

Accepted 11 March 2024

Available online 13 March 2024

Keywords:

Exome sequencing

FIG4

Osteopenia

VAC14

Yunis-Varón syndrome

ABSTRACT

Purpose: Biallelic variants in *FIG4* or *VAC14* are associated with Yunis-Varón syndrome (YVS), which is characterized by multisystem involvement including skeletal findings, craniofacial dysmorphisms and central nervous system anomalies. Pathogenic variants in those same genes have also been associated with a predominantly neurological phenotype and with nonsyndromic conditions, such as Charcot-Marie-Tooth disease and amyotrophic lateral sclerosis. By describing 5 new cases of *FIG4*-associated YVS and reviewing the literature, we better delineate the clinical phenotype associated with loss of function of those genes. We also explore osteopenia mechanisms by assessing bone physiologic parameters in a mouse model.

Methods: Exome sequencing or Sanger sequencing was performed in 5 unrelated individuals. Bone histomorphometry was performed in *Fig4*^{plv/plv} mice and compared with wild type. Relevant literature from the last 10 years was reviewed.

Results: All individuals presented a phenotype overlapping the typical YVS and the brain anomalies and neurologic syndrome. Clinical features included developmental delay, structural brain malformations, and skeletal anomalies, such as osteopenia. Biallelic *FIG4* variants were identified in each individual. In mice, bone histomorphometry parameters suggested that osteopenia might be secondary to reduced bone formation rather than increased bone degradation.

Conclusion: This study contributes to a better understanding of the phenotypic variability caused by pathogenic variants in *FIG4* or *VAC14* and suggests an important overlap between previously described phenotypes. The brain anomalies and neurologic syndrome is likely in the same spectrum as classical YVS. Further studies are still needed to clarify the effects of partial loss-of-function (hypomorphic) variants and to identify genotype-phenotype correlations.

© 2024 The Authors. Published by Elsevier Inc. on behalf of American College of Medical Genetics and Genomics. This is an open access article under the CC BY-NC-ND license (<http://creativecommons.org/licenses/by-nc-nd/4.0/>).

This article was invited and the Article Publishing Charge (APC) was waived.

Éliane Beauregard-Lacroix and Alexandra Scott contributed equally to this article.

*Correspondence and requests for materials should be addressed to Philippe M. Campeau, Department of Pediatrics, University of Montreal, Medical Genetics Service, Room 6727, Sainte-Justine Hospital, 3175, Cote-Sainte-Catherine, Montreal, QC, Canada H3T 1C5. Email address: p.campeau@umontreal.ca

Affiliations are at the end of the document.

doi: <https://doi.org/10.1016/j.gimo.2024.101837>

2949-7744/© 2024 The Authors. Published by Elsevier Inc. on behalf of American College of Medical Genetics and Genomics. This is an open access article under the CC BY-NC-ND license (<http://creativecommons.org/licenses/by-nc-nd/4.0/>).

Introduction

FIG4 (HGNC:16873) and *VAC14* (HGNC:25507) genes encode proteins that form a multiprotein biosynthetic complex with *Fab1/PIKfyve* (HGNC:23785), a lipid kinase adding a phosphate group to phosphatidylinositol 3 phosphate PI(3)P. This complex is localized at the membranes of late endosomes and lysosomes and modulates the level of phosphatidylinositol 3,5-bisphosphate (PI(3,5)P₂), a signaling molecule that plays an important role in protein sorting, endolysosomal vesicles trafficking and fusion at the cytoplasmic membrane, and other essential functions of endolysosome, such as cellular osmoregulation via regulation of ion channels. *FIG4* encodes the phosphatidylinositol phosphatase part of the complex, whereas *VAC14* encodes the scaffold protein of the complex, and they both function as an activator of *Fab1/PIKfyve*.¹⁻⁶

FIG4 or *VAC14* deficiency results in a significant reduction in PI(3,5)P₂^{2,4,7,8} and in PI(5)P, a lipid signaling molecule playing a role in autophagy and endosomal maturation.⁸ Depletion of PI(3,5)P₂ causes intracellular accumulation of enlarged endolysosomal vacuoles.^{2-4,7} In mouse models and human cells of individuals with partial or complete loss of *FIG4* or *VAC14*, we can observe the accumulation of large vacuoles compatible with lysosome-derived swollen vesicles in different tissues, such as skeletal muscles, fibroblasts, central nervous system (CNS) tissues (cortex, cerebellum, and basal ganglia),^{3,5,9-14} and calvarial tissue.⁹ Mouse models with homozygous variants of *FIG4* or *VAC14* display neurodegeneration and hypomyelination.^{2,9,12,14,15} *FIG4*-null mice also have reduced body weight and bone density, as well as vacuolated osteoblasts.⁹ As such, *FIG4-VAC14*-related disorders are considered by some to be part of the large group of lysosomal diseases.^{9,10,12,16} Neuronal expression of an enzymatically inactive *FIG4* in null mice (Plt mice used here, which do not express *FIG4*) does partially rescue the phenotype potentially by stabilizing the complex, but the neurological disease nevertheless progresses until an early death.¹⁷

In humans, partial loss-of-function variants in *FIG4* were first associated with the autosomal recessive Charcot-Marie-Tooth disease type 4J (CMT4J) (OMIM 611228) and the autosomal dominant amyotrophic lateral sclerosis type 11 (OMIM 612577). In the last decade, a wide spectrum of other autosomal recessive syndromes has been reported to be caused by partial or complete loss-of-function variants in *FIG4* gene, such as Yunis-Varón syndrome (YVS) (OMIM 216340), bilateral temporooccipital polymicrogyria syndrome (OMIM 612691), and cerebral hypomyelination.¹⁰ Loss-of-function variants in *VAC14* have been associated with striatonigral degeneration syndrome (OMIM 617054) and have been reported in a single individual with YVS.¹³ YVS is characterized by skeletal abnormalities (eg, aplasia/hypoplasia of clavicles and phalanges of hands and feet, absence of thumbs and halluces, pelvic bone dysplasia, and

ossification defects), craniofacial dysmorphisms, hypotrichosis, and structural brain anomalies with severe neurological disability. It is a very rare and severe condition, which is often lethal in infancy.¹⁸ Other more recently described phenotypes associated with a biallelic deficiency of *FIG4* or *VAC14* present with CNS anomalies and neurologic impairment as predominant features.^{10,12,19-25}

In this study, we present 5 individuals affected by *FIG4*-related autosomal recessive syndromes, in whom the spectrum of clinical manifestations is situated between the typical YVS and the brain anomalies and neurologic syndrome, and we review the literature of individuals with biallelic *FIG4* and *VAC14* variants to better delineate the clinical phenotypes associated with loss of function of those genes. We also explored osteopenia mechanisms by assessing bone physiologic parameters in a mouse model.

Material and Methods

The study was conducted according to the guidelines of the investigators' local institutional review board, and informed consent was obtained before collection of samples and pictures. The inclusion criterion was the identification of biallelic *FIG4* pathogenic or likely pathogenic variants, mostly in individuals with a high index of suspicion of YVS by a clinical geneticist.

DNA sequencing

Family 1 was consented for clinical exome sequencing. Exome sequencing was performed for the affected individual and both parents. Families 2, 3, and 4 consented to Sanger sequencing of the *FIG4* gene (RefSeq accession number NM_014845.6) in probands. Identified *FIG4* variants were afterward analyzed by Sanger sequencing in parents. In family 5, *FIG4* variant was identified through exome sequencing and was subsequently confirmed using Sanger sequencing in the affected individual and both parents.

Bone physiologic parameters

Fig4^{Plt/Plt} male mice were obtained from Dr Miriam Meisler and were sacrificed on day 21. Bone histology, staining, and histomorphometry were performed as previously described.²⁶⁻²⁸ Lumbar vertebrae were dissected, fixed for 24 hours in 10% formalin, dehydrated in graded ethanol series, and embedded in methyl methacrylate resin according to standard protocols. Von Kossa/Van Gieson and Goldner trichrome staining were used for bone volume and tissue volume measurements, whereas calcein double-labeling method²⁹ was used to analyze bone formation rate and mineralization apposition rate. For the analysis of osteoclasts, sections were stained with tartrate-resistant acid

phosphatase. Histomorphometric analyses were performed using the Osteomeasure Analysis System (Osteometrics).

Fibroblast study of *FIG4* variants

Skin fibroblasts were obtained from individual 1. After culture, light microscopy was performed.

Literature review

PubMed (<https://www.ncbi.nlm.nih.gov/pubmed/>) was used to search for studies from the last 10 years, using the keywords “VAC14” or “FIG4” and “syndrome.” A secondary search was performed by identifying pertinent articles cited in articles identified in the primary search.

Results

Clinical features of 5 affected individuals with *FIG4* variants

Individual 1 is a 6-year-old male. He was born at term with normal growth parameters. He presented with hypotonia and severe developmental delay. He also had one episode of seizure. Brain magnetic resonance imaging (MRI) showed dilation of the ventricles, cerebellar hypoplasia with hypoplastic vermis, severe global delayed myelination, and cervical canal stenosis. On physical exam, he was found with macrocephaly, wide anterior fontanelle, and protruding eyes with orbital fullness. Neurological exam revealed peripheral neuropathy with generalized weakness. Skeletal survey showed abnormal ossification of cranial vault, craniofacial disproportion, coxa valga, and osteopenia. Additional investigations revealed bilateral sensorineural hearing loss and dilated ascending aorta.

Individual 2 is a female, who was born small for gestational age with multiple anomalies. She had a cleft palate, genital anomalies, and limb anomalies with absent distal phalanges. Dysmorphic features included short philtrum with thin upper lip, micrognathia, and abnormal ears. She had severe developmental delay with hypotonia and seizures. She was fed exclusively through a gastrostomy and had severe failure to thrive. Brain MRI showed agenesis of corpus callosum, Dandy-Walker malformation, vermis hypoplasia, basal ganglia anomalies, and hypomyelination. Eye exam revealed bilateral retinopathy and normal cornea with some opacity of lens segment. Skeletal survey identified abnormal ossification of cranial vault, absent clavicles, coxa valga with hip subluxation, and osteoporosis. She gradually lost her ability to move and developed contractures but did not have spasticity or any movement disorder. She passed at 14 years of age.

Individual 3 is a 7-year-old female. Growth parameters were normal at birth. She was born with absent thumbs and

halluces. She also presented with hypotonia, severe developmental delay, and seizures. Brain MRI revealed pachygyria, Dandy-Walker malformation, cerebral atrophy, hypoplastic vermis, basal ganglia anomalies, and hydrocephalus (Figure 1B-D). Skeletal survey showed abnormal ossification of cranial vault, absent clavicles, hip dislocation, absent distal phalanges, and osteopenia (Figure 1E). She had cortical cataract, bilateral retinal detachment, and bilateral sensorineural hearing loss. Neurological exam confirmed the presence of lower limbs spasticity and peripheral neuropathy.

Individual 4 is a male who was born at 36 3/7 weeks of gestation with hypotonia and abnormal thumbs and halluces. Birth weight was on the 3rd percentile and head circumference was on the 1st percentile, whereas length was on the 13th percentile for his gestational age. He had several dysmorphic features, including protruding eyes, anteverted nares, short philtrum, high-arched palate, micrognathia, low-set and dysplastic ears, and hypoplastic nipples (Figure 1A). He also had sparse scalp hair and absent eyebrows and eyelashes. On brain MRI, he was found with absent olfactory bulbs and tracts, hypomyelination, cerebral atrophy, and vermis hypoplasia. Skeletal survey showed abnormal ossification of cranial vault with widened fontanelle, absent clavicles, pelvic dysplasia, and hypoplastic middle and distal phalanges (Figure 1F-I). Eye exam revealed bilateral congenital cataract. He also had hearing loss. He passed at 1 month of age.

Individual 5 is a 14-year-old male. He presented with mild intellectual disability and a complaint of lower limbs weakness. Physical exam revealed microcephaly, low columella, short and broad thumbs and halluces, and brittle, thick, and discolored hair. Brain MRI and skeletal survey were not performed.

Molecular analysis of *FIG4* variants

The *FIG4* genotypes of parents and affected offspring in the 5 families described in Table 1 are shown in Figure 2. Figure 2 shows notably the catalytic site of *FIG4*, in brown. Note that the first third of *FIG4* is important for its interaction with VAC14. Individual 3 has missense variants in both regions. Supplemental Table 1 shows American College of Medical Genetics and Genomics classification of the variants.

All alleles were in trans, confirming the autosomal recessive inheritance of the disorder (Figure 2A). In family 1, the affected individual is the first and only male child of a nonconsanguineous couple. The mother is heterozygous for a nonsense variant c.1141C>T p.(Arg381*), and the father has a donor splice site variant c.2459+1G>A (see Figure 2A and B). The nonsense variant p.(Arg381*) was first described in CMT4J, an autosomal recessive peripheral neuropathy with severe motor dysfunction and rapid progression, and is considered a null allele because it is predicted to cause nonsense mediated decay (NMD).³⁰ It is

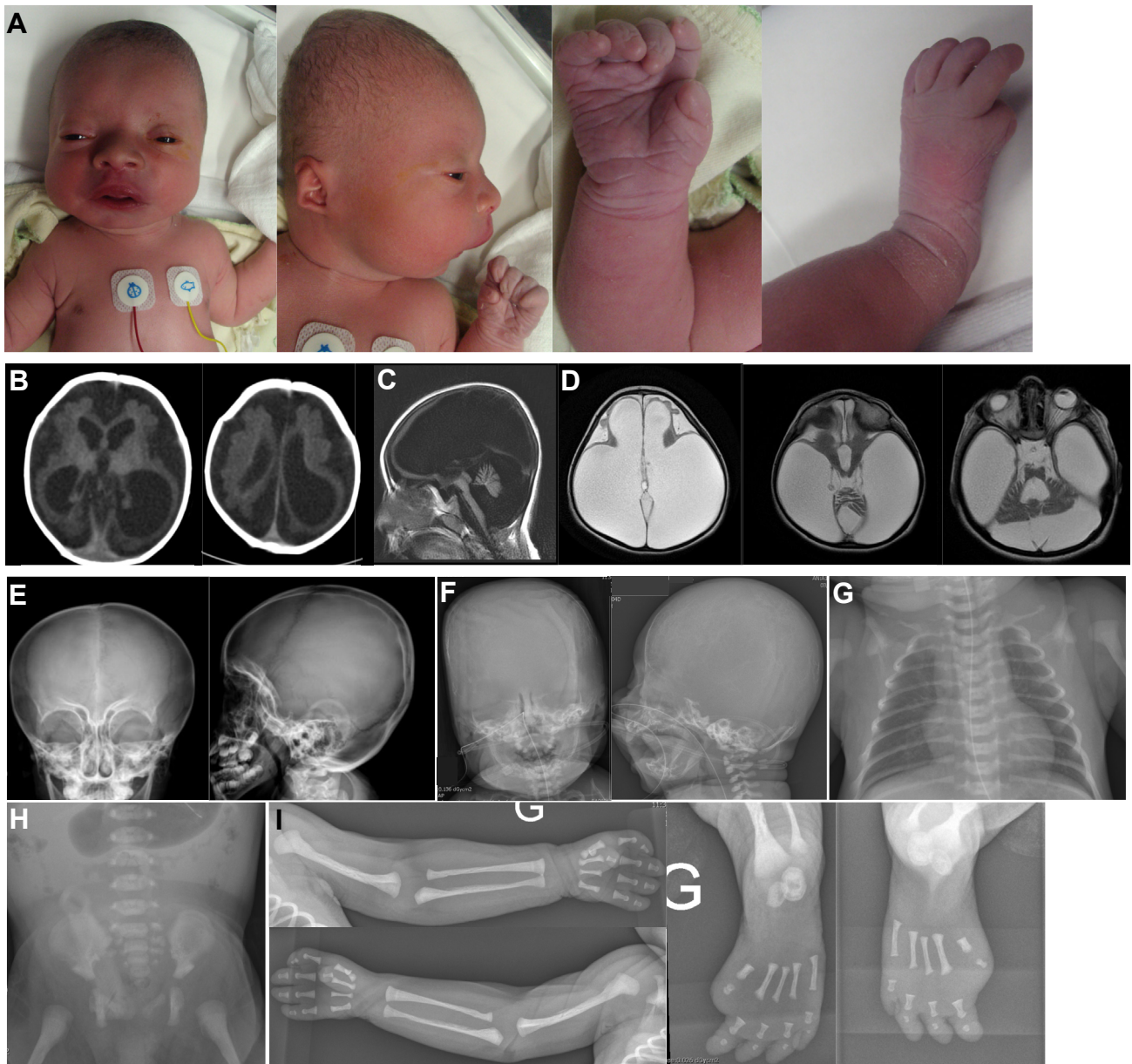


Figure 1 Photographs, brain imaging and X-rays of affected individuals. A. Individual 4. Note microcephaly, sparse scalp hair, absent eyebrows and eye lashes, protruding eyes, anteverted nares, short philtrum, micrognathia, low-set dysplastic ears with brachydactyly, thumb and hallux hypoplasia, and hypoplastic nails. B-D. Brain imaging of individual 3. B. CT axial: diffuse pachygyria with ventricular dilatation more significant at the left ventricle. C. MRI axial T2: frontal bilateral pachygyria, extreme bilateral ventricular dilatation, IV ventricle dilatation, thinned mesencephalus, atrophic cerebellum, and thinned thalamus. D. MRI sagittal T1: “J-shaped” sella, thinned cerebral cortical parenchyma and Dandy-Walker malformation. E and F. Skull X-ray, frontal and lateral plane of individuals from family 3 (E) and family 4 (F). Note unmineralized skull and craniofacial disproportion. G. Chest Radiograph showing narrow chest and hypoplastic clavicles in individual from family 4. H. Plain abdominal X-ray showing pelvic dysplasia in individual from family 4. I. Upper limb X-ray of individual 4 showing complete absence of thumb, hypoplasia of halluces, and hypoplastic middle and distal phalanges.

furthermore localized in the Sac1 homology domain-containing inositol phosphatase and upstream of the phosphatase catalytic motif CX5RT/S; therefore, even if NMD is incomplete, complete loss of enzymatic function of the protein is expected.^{9,31} The splice site variant c.2459+1G>A was previously described in 3 affected individuals with cerebral hypomyelination and neurologic syndrome.¹⁰ It is a rare variant in the general population

(allele frequency of 0.00000797 in gnomAD³²). The variant is expected to be a loss-of-function allele because the G>A substitution at the consensus +1 position of intron 21 most probably disables the donor splice site of exon 21 according to protein prediction programs (Supplemental Results 2) and RNA studies demonstrated that the subsequent read-through into intron 21 generates a unique shorter RNA product that lacks hundreds of C-terminal

Table 1 Clinical features of FIG4 variant positive patients in this study

Clinical Characteristics	Family 1	Family 2	Family 3	Family 4	Family 5	Review of the Literature (n = 30 ^a)
<i>FIG4</i> variants (NM_014845.6, NP_055660.1, NC_000006.12)	c.1141C>T, p.(Arg381*), g.109760253C>T (mat); c.2459+1G>A, g.109792665G>A (pat)	c.1294C>T, p.(Arg432*), g.109762113C> T(homozygous)	c.122T>C, p.(Ile41Thr), g.109715133T>C (mat); c.1474C>T, p.(Arg492Cys), g.109765052C>T (pat)	c.2285_2286del, p.(Ser762Trpfs*3), g.109791480_ 109791481del (homozygous)	c.1583+1G>T, g.109765162G> T (homozygous)	
Consanguinity	—	—	+ (first cousins)	—	+ (first cousins)	
Gender	M	F	F	M	M	
Postnatal evolution	6 years at last follow-up	Deceased at 14 years	7 years at last follow-up	Deceased at 1 month	14 years at last follow-up	
GROWTH						
Prenatal growth retardation	—	+	—	—	—	
Birth weight (g)	4024	2476	3280	2480	NA	2448 ± 908
BW < 3e centile	—	+	—	—	NA	13/30 (43%)
Birth length (cm)	54	NA	51	47	NA	46 ± 7
BL < 3e centile	—	NA	—	—	NA	12/27 (44%)
OFC at birth (cm)	NA	34	32.5	31	NA	31 ± 5
Severe postnatal failure to thrive	—	+	—	NA	—	4/6 (67%)
Microcephaly	—	—	—	+	+	15/29 (52%)
HEAD and NECK						
Sparse scalp hair	—	—	—	+	—	27/29 (93%)
Absent eyebrows and eyelashes	—	NA	—	+	—	6/7 (86%)
Widened fontanelle/sutures	+	NA	—	+	—	26/28 (93%)
Protruding eyes	+	—	—	+	—	20/25 (80%)
Corneal opacity/congenital cataract	—	+	+	+	—	11/28 (39%)
Anteverted nares	—	—	—	+	—	20/26 (77%)
Short philtrum	—	+	—	+	—	10/20 (50%)
Short upper lip	—	+	—	—	—	20/26 (77%)
Labiogingival retraction	—	NA	—	—	—	13/22 (59%)
High arched palate	—	+ (cleft palate)	—	+	—	15/22 (68%)
Micrognathia	—	+	—	+	—	13/14 (93%)
Low-set/dysplastic ears	—	+	—	+	—	30/30 (100%)
Loose nuchal skin	—	NA	—	+	—	13/15 (87%)
Hearing lost	+	—	+	+	—	4/13 (30%)
THORAX						
Congenital heart defect	+ (dilated ascending Ao)	—	—	—	—	5/14 (36%)
Absent/hypoplastic nipples	—	—	—	+	—	5/20 (25%)
GENITOURINARY						
Genital anomalies	—	+	—	—	—	9/26 (35%)
LIMBS						
Absent/hypoplastic thumbs	—	+	+	+	+	28/30 (93%)

(continued)

Table 1 Continued

Clinical Characteristics	Family 1	Family 2	Family 3	Family 4	Family 5	Review of the Literature (n = 30 ^a)
Absent/hypoplastic halluces	–	+	+	+	+	27/29 (93%)
Nail aplasia/hypoplasia	–	+	+	+	–	24/26 (92%)
Single transverse palmar creases	–	NA	–	NA	NA	10/15 (67%)
RADIOLOGICAL						
Abnormal ossification of cranial vault	+	+	+	+	NA	21/26 (81%)
Osteoporosis	osteopenia	+	osteopenia	NA	NA	8/27 (30%)
Absent/hypoplastic clavicles	–	+	+	+	NA	16/19 (84%)
Craniofacial disproportion	+	–	–	–	–	19/26 (73%)
Absent sternal ossification center	–	–	–	–	NA	9/12 (75%)
Pelvic dysplasia	+	+	–	+	NA	16/21 (76%)
Hip dislocation	–	+	+	–	NA	9/19 (47%)
Aplastic/hypoplastic middle phalanges	–	+	–	+	NA	20/26 (77%)
Aplastic/hypoplastic distal phalanges	–	+	+	+	NA	22/24 (92%)
CENTRAL NERVOUS SYSTEM (n = 58 ^b)						
Retinopathy	–	+	+	+	NA	5/25 (20%)
Structural brain anomalies	+	+	+	+	NA	34/45 (76%)
Agenesis/hypoplasia of corpus callosum	–	+	–	–	NA	3/33 (9%)
Absent olfactory bulbs and tracts	–	–	–	+	NA	1/33 (3%)
Pachygyria or polymicrogyria (temporo-occipital)	–	+	+	+	NA	5/33 (15%)
Dandy–Walker malformation	–	+	+	–	NA	1/33 (3%)
Leukodystrophy/hypomyelination	+	+	–	+	NA	8/33 (24%)
Cerebral or cerebellar/white matter atrophy	+	–	+	+	NA	8/33 (24%)
Vermis hypoplasia	+	+	+	+	NA	4/33 (12%)
Basal ganglia anomalies	–	+	+	–	NA	10/33 (30%)
Ventriculomegaly	+	–	+	–	NA	4/33 (12%)
Hypointense substantia nigra	–	–	–	–	NA	4/33 (12%)
Severe developmental delay	+	+	+	+	–	30/40 (75%)
Hypotonia	+	+	+	+	–	23/45 (51%)
Speech difficulties (eg, dysarthria)	–	+	+	NA	–	14/28 (50%)
Movement disorder (eg, ataxia, dystonia, chorea, etc.)	–	+	+	NA	–	18/28 (64%)
Peripheral neuropathy	+	–	+	NA	–	7/27 (26%)
Seizures	+	+	+	–	–	6/29 (21%)
LABORATORIES (n = 58 ^b)						
Enlarged cytoplasmic vacuoles	+	+	NA	NA	NA	14/17 (82%)

Plus signs (+) and minus signs (–) indicate presence and absence of trait, respectively.

Ao, aorta; BL, birth length; BW, birth weight; F, female; M, male; OFC, occipitofrontal circumference; NA, not assessed.

^aYunis-Varon syndrome patients in the literature.

^bFIG4-VAC14 variant positive patients in the literature with Yunis-Varon syndrome (n = 30) or Brain anomalies and neurologic syndrome (n = 28).

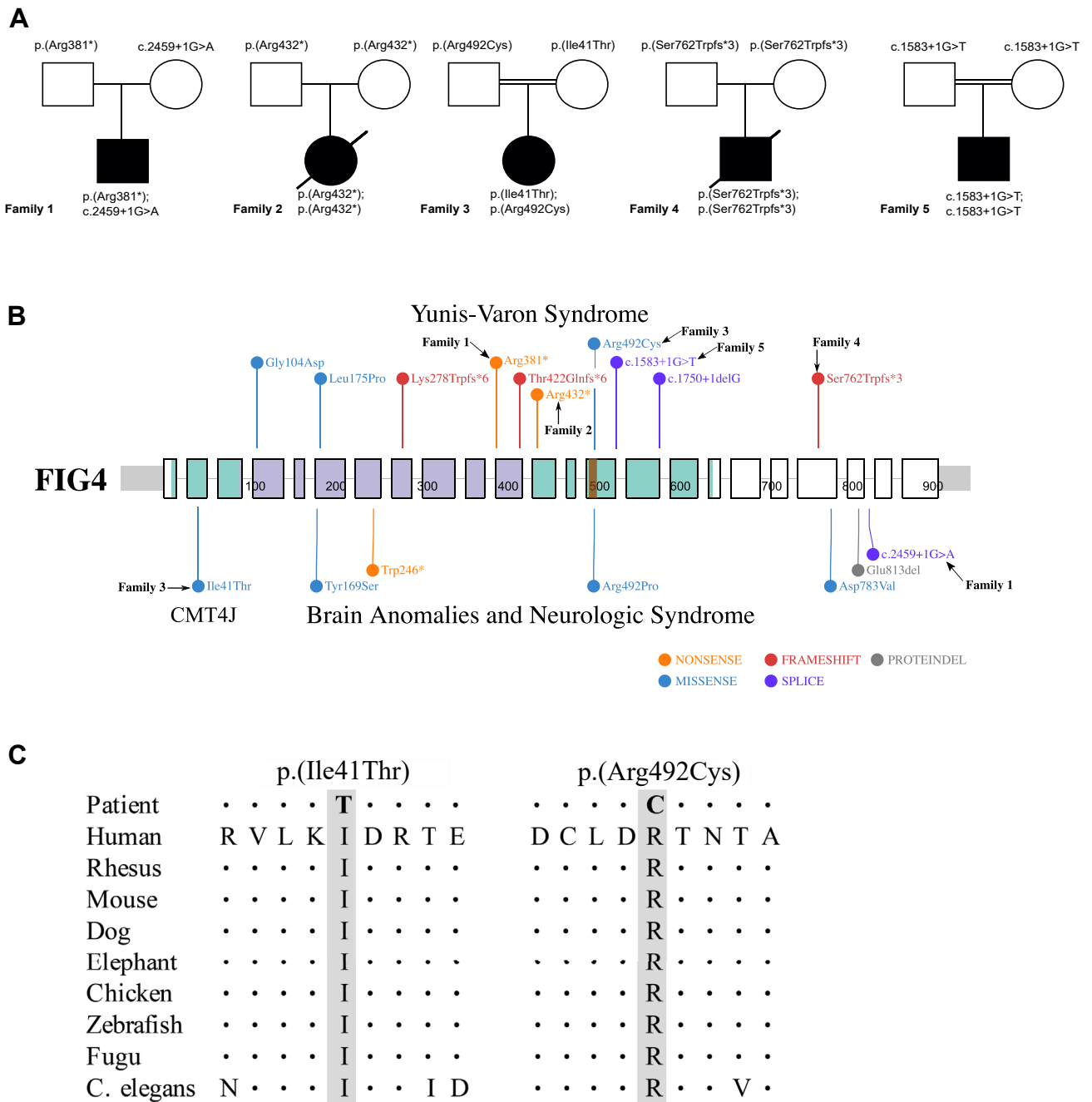


Figure 2 Segregation of *FIG4* variants in 5 families and location of *FIG4* variants. A. *FIG4* genotypes of family members demonstrating autosomal recessive inheritance. Numbering from RefSeq NM_014845.5. B. Location of variants in *FIG4* exons; introns not drawn to scale. Above, YVS; below, Brain anomalies and neurologic syndrome. Phosphoinositide polyphosphatase domain, green; Sac1 homology domain-containing inositol phosphatase, purple; P loop containing the catalytic CX5R(T/S) motif, orange. Arrows point to *FIG4* variants reported in this study. C. Evolutionary conservation of amino acids around the missense variants. Dots represent identity.

residues compared with the wild-type protein.¹⁰ SpliceAI also predicts a donor loss with a delta score of 1. The C-terminal domain docks the *FIG4* protein to the membranes³¹ and binds VAC14 to the complex.⁴ Some consider that a C-terminal truncated protein will keep partial function because the phosphatase domain and the catalytic active site are retained.^{4,10}

In family 2, the parents are not related, but both are heterozygous for the same nonsense variant c.1294C>T p.(Arg432*) (Figure 2A and B). The c.1294C>T variant is rare (allele frequency of 0.00000796 in gnomAD³²) and predicted pathogenic by multiple protein prediction programs, most probably by causing NMD. Even if NMD was incomplete, it is an enzymatic null allele because the

nonsense variant is localized in the phosphoinositide polyphosphatase domain and upstream of the phosphatase catalytic motif CX5RT/S and therefore will lead to complete loss of function of the protein.^{9,31}

In family 3, the individual is the only female child of first cousins, but each parent is heterozygous for a different variant. The mother is heterozygous for the missense variant c.122T>C p.(Ile41Thr), the common pathogenic missense variant reported in CMT4J,³⁰ whereas the father is heterozygous for a novel missense variant c.1474C>T p.(Arg492Cys) (Figure 2A and B). Both missense variants concern amino acid residues highly conserved through evolution (Figure 2C). The p.(Ile41Thr) is a very well-described variant encountered in CMT4J. This missense substitution is predicted to cause partial loss of function of the protein by reducing the binding affinity of FIG4 for the scaffold protein VAC14 and for Fab1/PIKFYVE (the substitution is located at the N-terminal surface of FIG4 that contains the VAC14 binding domain and plays an important role in *Fab1* activation⁴). Therefore, it disrupts to a certain extent the multiprotein biosynthetic complex and causes low protein level in functional studies.^{4,9,11,30} The missense variant inherited from the father, p.(Arg492Cys), has not been previously reported, but it affects a highly conserved amino acid residue positioned in the phosphatase catalytic active site (in the motif CX5RT/S). Therefore, the arginine for cysteine substitution at this position is expected to destabilize the dephosphorylation transition state and modify *Fab1* association with the complex,⁴ consequently occasioning complete loss of enzymatic activity of the multiprotein complex.^{10,31}

In family 4, the parents are nonconsanguineous, but both are heterozygous for the same 2 bp frameshift deletion c.2285_2286del p.(Ser762Trpfs*3) (Figure 2A-B). It is predicted to cause loss of function of the protein as a frameshift truncating variant, the altered protein lacking the C-terminal residues of the wild-type protein that anchor the FIG4 protein to membranes^{9,31} and that stabilize the binding of VAC14 to the complex.⁴ This variant was reported as a null allele in a previous study, for an individual with YVS,³³ but it can be argued that the loss of function may be partial as the protein will retain the phosphoinositide phosphatase domain and the catalytic active site.^{4,10} The severity of individual 4's phenotype could suggest that this variant causes a complete loss of function of the protein, but it is also possible that additional factors could contribute to his phenotype.

In family 5, the affected individual is homozygous for the splice variant c.1583+1G>T. His parents are first cousins. He has a younger unaffected sister who was found heterozygous for the same variant. It is a rare variant that is absent from populational database gnomAD³² and has never been reported in the literature. It affects a donor splice site (Supplemental Material 2) and is therefore predicted to result in a loss of function. SpliceAI, indeed, predicts a donor loss with a delta score of 1. However, because there are no functional data for this specific variant, its consequence on the protein remains uncertain.

Bone physiologic parameters

Given the osteopenia and osteoporosis noted in YVS and the reduced bone density we previously reported in mice, we aimed to better understand that mechanism underlying these observations. Mice vertebrae histology analysis showed that bone surface/bone volume fraction and bone volume/tissue volume fraction were significantly decreased in *Fig4^{plv/plv}* mice compared with *Fig4^{+/+}* mice. Marrow volume fraction was increased. Trabecular number was reduced, whereas trabecular separation was increased. There was no statistically significant difference for trabecular thickness (Figure 3B). Tartrate-resistant acid phosphatase staining for osteoclasts revealed no statistically significant difference either (Figure 3C). Mineralizing surface and bone formation rate were reduced in *Fig4^{plv/plv}* mice (Figure 3E). Overall, those findings suggest that osteopenia in YVS might be secondary to slower bone formation rather than increased bone resorption.

Fibroblast study of FIG4 variants

To further highlight the vacuolation abnormalities in YVS, we studied fibroblasts of individual 1. Light microscopy revealed the presence of enlarged vacuoles (Figure 3F), which is in accordance with results from previous studies.^{3,9,10,12}

Literature review of FIG4-VAC14-related disorders

A total of 30 cases of Yunis-Varón syndrome^{9,13,16,33-41} and 28 cases of brain anomalies and neurologic syndrome^{2,11,20,24,25,30,34,36,37} were retrieved from the literature, either having biallelic *FIG4* variants,^{9,10,19,24,25,33,41} biallelic *VAC14* pathogenic variants,^{5,12,13,20-23} or unknown genotype.^{9,16,34-40} YVS cases included only 1 individual with *VAC14* variants (the remaining being either *FIG4* variants or unknown genotype), whereas the neurological phenotype was associated with *FIG4* variants in 17 cases and *VAC14* in 11 cases. The clinical features of the YVS individuals are summarized in Supplemental Table 3 and clinical features of individuals with brain anomalies and a neurologic syndrome are compiled in Supplemental Table 4.

Regarding YVS (Supplemental Table 3), the most frequent craniofacial clinical features described in the literature (>70% of cases) are protruding eyes, anteverted nares, short upper lip, high-arched or cleft palate, micrognathia, low-set and dysplastic ears, and hypotrichosis (hair, eyebrows, and eyelashes). Less-frequent recurrent craniofacial features not previously mentioned stand out of the literature review, namely, sensorineural hearing loss (30% of cases) and corneal opacity or congenital cataract (39% of cases). These findings were found retrospectively in many cases previously reported.

Recurrent skeletal features (>75% of cases) involve widened fontanelle or sutures, calvarial dysostosis, digital

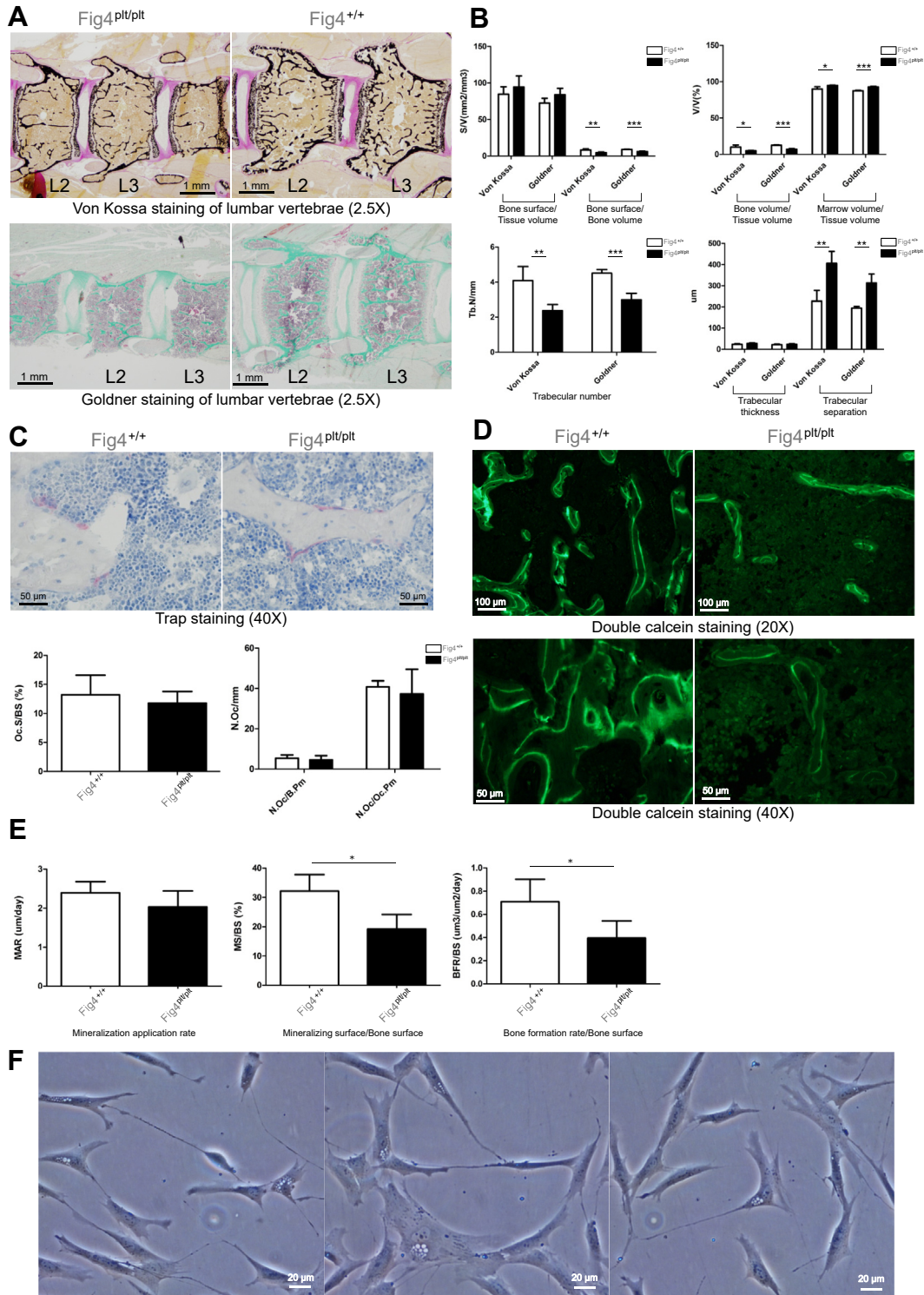


Figure 3 Bone Physiologic Parameters and Abnormal Subcellular Morphology in *FIG4* mutated fibroblasts. A. Von Kossa and Goldner staining of lumbar vertebrae in *Fig4^{plv/plv}* and *Fig4^{+/+}* mice. B. Vertebral bone parameters. S/V, surface/volume; V/V, volume/volume; Tb.N, trabecular number; * $P < .05$; ** $P < .01$; *** $P < .001$. C. Tartrate-resistant acid phosphatase staining in *Fig4^{+/+}* and *Fig4^{plv/plv}* mice. Oc.S/BS, osteoclast surface/bone surface; N. Oc, osteoclast number. D. Double calcein staining in *Fig4^{+/+}* and *Fig4^{plv/plv}* mice. E. Mineralization application rate (MAR), mineralized surface (MS/BS) and bone formation rate (BFR). * $P < .05$. F. Light microscopy of cultured skin fibroblasts from individual 1 showing large, empty cytoplasmic vacuoles.

hypoplasia with or without nail aplasia or hypoplasia, most frequently involving the thumbs, halluces, and distal phalanges, absent or hypoplastic clavicles, and pelvic dysplasia

and/or hip dislocation. Osteoporosis/osteopenia was not previously noted but is present in 30% of cases. This feature is consistent with *FIG4*-null mouse model reported in

Campeau et al.⁹ that has bone trabeculation, volume, surface, thickness, and density reduced by more than 50% compared with the wild-type mouse. Note that the patients described here were not treated with bisphosphonates because they did not have recurrent fractures.

Two-thirds of the affected individuals from the literature also presented with severe neurological manifestations: severe developmental delay and CNS anomalies, such as agenesis/hypoplasia of corpus callosum, cerebral (white matter) atrophy, vermis hypoplasia, basal ganglia anomalies, ventriculomegaly, and pachygyria. Moreover, 88% of YVS were significantly hypotonic.

Cardiac defects seem to be more prevalent than previously thought (36% vs 20% in a previous report⁹). On the other hand, prenatal growth retardation is less frequent than previously assessed (BL < 3e centile in 44% of cases vs 59% in a previous review⁹ and BW < 3e centile in 43% of cases vs 71% in a previous report⁹). Severe failure to thrive is noted in 67% of survivors, and microcephaly is present in 52% of affected individuals. Fifty percent of cases from the literature exhibit enlarged cytoplasmic vacuoles in cultured cells.

Concerning the brain anomalies and neurologic syndrome (Supplemental Table 4), the predominant clinical features noted in the literature are severe developmental delay (79% of cases) and CNS anomalies (85% of cases), such as leukodystrophy/hypomyelination, polymicrogyria (for individuals with *FIG4* variants), basal ganglia anomalies, and hypointense substantia nigra (for individuals with *VAC14* variants) with usual onset in early childhood. Less-frequent recurrent clinical manifestations include movement disorders, such as dystonia, rigidity, ataxia, spasticity (64%), speech difficulties (50%), hypotonia (29%), peripheral neuropathy (26%), seizures (21%), retinopathy (20%), and mild skeletal anomalies, such as coxa valga, hip dislocation, abnormal trabeculations in bones,^{10,24} and brachydactyly (27%). One hundred percent of cases from the literature that had a cultured cell analysis exhibit enlarged cytoplasmic vacuoles in those cells. Individuals with biallelic *VAC14* variants also present with developmental regression and (rapidly) progressive neurodegeneration.²¹

Discussion

According to recent studies,^{9,10,24,33} depending on the combination of allelic variants of *FIG4* gene and the degree of residual function of *FIG4* protein or level of remaining protein, affected individuals will suffer diverse clinical consequences, namely, complete loss of *FIG4* activity as a result of biallelic null variants is expected to cause the most severe phenotype of YVS,^{9,33} whereas compound heterozygous variants comprising a null allele and an hypomorphic allele or 2 partial loss-of-function alleles lead to a phenotype limited to the nervous system, such as the less severe phenotype of Charcot-Marie-Tooth type 4J (only peripheral nervous system)³⁰ or such as the intermediate phenotype of brain anomalies and neurologic syndrome

(central and peripheral nervous system).^{10,24} A similar interpretation can be retrieved in *VAC14*-related disorders.¹² In this study, individuals 2 and 4 seem to correspond to that model, both having biallelic predicted null variants and a more severe phenotype, with the classical clinical features of YVS. Individual 4 has, indeed, the most complete and severe YVS phenotype and had besides the most severe clinical course, with death at 1 month, although his homozygous variant can be considered a partial loss-of-function variant according to a certain interpretation of the variant pathogenicity (see Molecular analysis of *FIG4* variants).

However, from our analysis, the clinical consequences of the combination of a predicted partial loss-of-function variant with a predicted null variant seem to be much more diversified than previously expected. Some individuals display a peripheral neuropathy (CMT4J), especially when the missense variant p.Ile41Thr is involved,^{10,30} some have brains anomalies with neurological manifestations, including peripheral neuropathy,^{10,12,19,24} but others exhibit a mixture of neurologic features from the 2 above-mentioned neurologic disorders and the typical craniofacio-skeletal features of YVS,¹⁰ as individuals 1 and 3 from this study. Thus, individual 1 has a severe neurologic presentation with severe developmental delay, significant hypotonia, seizures, peripheral neuropathy causing diffuse muscle weakness, bilateral sensorineural hearing loss, multiple brains anomalies, ranging from myelination abnormalities to cortical atrophy, cerebellar anomalies, and ventriculomegaly with macrocephaly but also demonstrates important skeletal features, such as osteopenia, widened fontanelle and sutures, abnormal ossification of the cranial vault, craniofacial disproportion, cervical canal stenosis due to vertebral subluxation and coxa valga, and a congenital heart defect (dilated ascending aorta). Concerning individual 3, her clinical phenotype is even more interesting because she has the common missense variant p.Ile41Thr only previously described in most individuals with CMT4J³⁰ in trans with a null allele but still presents with many frequent skeletal features of YVS, such as abnormal ossification of the cranial vault, osteoporosis, hypoplastic clavicles, digital hypoplasia, and nail hypoplasia, as well as corneal opacity and bilateral sensorineural hearing loss, in addition to her severe neurologic manifestations of significant developmental delay, hypotonia, seizures, peripheral neuropathy (as in CMT4J), and multiple brain anomalies (Figure 1C-E).

Individual 5 is homozygous for a splice variant and appears to have a less severe phenotype with minimal skeletal involvement and mild cognitive impairment. It suggests that the variant does not cause a complete loss of function but would instead result in a protein with a partial function. Functional studies would be needed to formally assess consequences of the variant.

Other overlaps between the OMIM phenotypes can be observed when comparing the affected individuals from this study and the cases from the literature. For example, many of the structural brain anomalies of YVS overlap with the

brain anomalies and neurologic syndrome, such as polymicrogyria or pachygyria, basal ganglia anomalies, leukodystrophy/hypomyelination, or white matter atrophy. The presence of white matter atrophy and hypomyelination reinforces the potential role of FIG4-VAC14-multiprotein complex in myelin biosynthesis.^{12,15}

The clinical heterogeneity between individuals with a predicted null allele and a predicted partial loss-of-function allele is striking. The question remains if it could be related to the specific hypomorphic variant, which does not seem to be the case (eg, individual 2 with the classic CMT4J missense variant), or if modifier genes play an important role in this variable expressivity. It also raises the question whether skeletal anomalies and other malformations were not assessed frequently enough in cases from the literature when the phenotype was predominantly neurologic. On the other hand, peripheral neuropathy, movements disorder, or seizure were present in most of the affected individuals in this study, but they are usually associated with the brain anomalies and neurological syndrome and were not described in the YVS cases from the literature. The absence of these clinical manifestations in previously reported YVS individuals can probably be explained by the fact that these features were not investigated or not possible to assess because of the severe central neurological presentation of these individuals and/or their frequent early death.⁹ These neurological findings can now be considered part of the YVS phenotype as well. The same goes for retinopathy because individual 2 from this study displayed this retinal disorder while she had a typical YVS phenotype. Thus, we consider that individuals with partial loss-of-function variants in *FIG4*, and an apparently isolated peripheral nervous system phenotype should be investigated for CNS anomalies, and individuals with partial loss-of-function variants in *FIG4* or *VAC14* with a predominantly CNS phenotype should be assessed systematically for skeletal anomalies, congenital heart defect, and other craniofacial features, such as eye anomalies (cataract, retinopathy, etc) and deafness. Moreover, seizures, neuropathy, movement disorders, and retinopathy should be assessed systematically in YVS individuals.

We should consider that CMT4J, brain anomalies and neurologic syndrome, and YVS are part of the same phenotypic continuum.^{10,21,24} As we can see from the literature review, individuals with *VAC14* or *FIG4*-deficiency display a very similar spectrum of phenotypes. As such, we argue that these 2 genes share the same spectrum of clinical syndromes, which is concordant with their tightly associated roles in the same multiprotein complex. We can now talk about a spectrum of *FIG4*-*VAC14*-related disorders.^{10,21,24}

It is important to note that most of the participants from this study survived beyond 6 years of life, contrary to cases from the literature who frequently died in infancy, usually from respiratory complications (Supplemental Table 3), except for 6 individuals from the literature for whom we

have data beyond infancy.^{9,35} This widens the life expectancy of YVS individuals.

Finally, we highlight that 30% of the patients have osteopenia or osteoporosis and explored this aspect in a mouse model. Indeed, osteopenia or osteoporosis can be secondary to an imbalance between bone formation and bone degradation. Here, we show that although the osteoclasts are normal, there is however reduced bone formation, which is consistent with our previous observation of large vacuoles in mouse osteoblasts. Thus, we can ascertain that the mechanism of osteopenia and osteoporosis in YVS is through osteoblast dysfunction. Should fractures be recurrent in affected individuals, bisphosphonates could be used to inhibit osteoclasts and try to rebalance bone metabolism.

In summary, this study contributes to a better understanding of the phenotypic variability related to pathogenic and likely pathogenic variants in *FIG4* or *VAC14*, suggesting an important overlap between the previously described phenotypes and that not only null variants can cause a YVS clinical presentation. Individuals with *FIG4* or *VAC14* biallelic variants should be investigated for CNS anomalies, peripheral neuropathies, seizures, eye anomalies, deafness, skeletal malformations, and congenital heart defect as part of the evaluations after initial diagnosis. Enlarged vacuoles of lysosomal origin in cultured cells is a recurrent marker of the impaired function of *FIG4* and *VAC14* proteins.^{5,9,10,12,13} Osteopenia is a recurrent finding in YVS individuals and, according to analyses performed on mouse models, it seems to be due to reduced bone formation rather than increased bone resorption. Further experiments could explore the osteoblasts pathways affected by lysosomal dysfunction.

The genotype-phenotype correlation still needs further studies to clarify the effects of partial loss-of-function variants, for example, by measuring enzymatic activity resulting from the hypomorphic alleles¹⁰ or to identify modifier genes that can affect the prognosis and clinical characteristics. To account for cases with unknown genotype, many YVS individuals from the literature haven't been tested for *FIG4* variants or *VAC14* variants. Yunis-Varón syndrome could also be more genetically heterogeneous than what has been reported by now.⁹ *Fab1/PIKFYVE* would be an interesting new candidate gene as part of the trimolecular protein complex with *VAC14* and *FIG4*.

Data Availability

All data generated or analyzed during this study are included in this article and its supplemental information files.

Acknowledgments

The authors thank Guy M. Lenk and Miriam H. Meisler for providing *Fig4*^{pl^l/pl^l} mice.

Funding

Funding was provided to Philippe M. Campeau by Clinician-Scientist Award from the Fonds de Recherche du Québec-Santé and from the Canadian Institutes of Health Research.

Author Information

Conceptualization: É.B.-L., A.S., T.T.M.N., M.F., P.M.C.; Formal Analysis: T.T.M.N.; Funding Acquisition: P.M.C.; Investigation: É.B.-L., A.S., T.T.M.N., M.F., P.M.C.; Methodology: T.T.M.N., M.F., P.M.C.; Project Administration: M.F., P.M.C.; Resources: K.J.W., G.P., A.B.K., D.R.C., J.-L.A., F.P., K.M.G., M.F., P.M.C.; Supervision: P.M.C.; Validation: T.T.M.N., M.F., P.M.C.; Visualization: É.B.-L., A.S., T.T.M.N., P.M.C.; Writing-original draft: É.B.-L., A.S., P.M.C.; Writing-review and editing: É.B.-L., A.S., T.T.M.N., K.J.W., G.P., A.B.K., D.R.C., J.-L.A., F.P., K.M.G., M.F., P.M.C.

Ethics Declaration

This project was approved by the institutional review board (IRB) of CHU Sainte-Justine. Written informed consent was obtained from all participants or their parents. Explicit permission was obtained to publish photos, when applicable.

Conflict of Interest

The authors declare no conflicts of interest.

Additional Information

The online version of this article (<https://doi.org/10.1016/j.gimo.2024.101837>) contains supplemental material, which is available to authorized users.

Affiliations

¹Medical Genetics Division, Department of Pediatrics, CHU Sainte-Justine, Montreal, QC, Canada; ²CHU Sainte-Justine Research Center, Université de Montréal, Montreal, QC, Canada; ³Department of Clinical Genomics, Mayo Clinic, Jacksonville, FL; ⁴University of Oklahoma Health Sciences Center, Oklahoma City, OK; ⁵Child Habilitation Unit, Akershus University Hospital, Nordbyhagen, Norway; ⁶Child Neurohabilitation Unit, Oslo University Hospital,

Oslo, Norway; ⁷Genetic Unit, SARAH Network of Rehabilitation Hospitals, Brasilia, Brazil; ⁸Pôle Femme-Mère-Enfants, CH Félix Guyon, CHU de La Réunion, Saint-Denis, La Réunion, France; ⁹Service de Génétique, CH Félix Guyon, CHU de La Réunion, Saint-Denis, La Réunion, France; ¹⁰Department of Medical Genetics, Kasturba Medical College, Manipal, Manipal Academy of Higher Education, Manipal, Karnataka, India; ¹¹Suma Genomics Private Limited, Manipal, India; ¹²Molecular Physiology Research Unit, Institut de Recherches Cliniques de Montréal, Montreal, QC, Canada; ¹³Department of Medicine, Université de Montréal, Montreal, QC, Canada

References

1. Botelho RJ, Efe JA, Teis D, Emr SD. Assembly of a Fab1 phosphoinositide kinase signaling complex requires the Fig4 phosphoinositide phosphatase. *Mol Biol Cell*. 2008;19(10):4273-4286. <http://doi.org/10.1091/mbc.e08-04-0405>
2. Jin N, Chow CY, Liu L, et al. VAC14 nucleates a protein complex essential for the acute interconversion of PI3P and PI(3,5)P(2) in yeast and mouse. *EMBO J*. 2008;27(24):3221-3234. <http://doi.org/10.1038/emboj.2008.248>
3. Sbrissa D, Ikononov OC, Fu Z, et al. Core protein machinery for mammalian phosphatidylinositol 3,5-bisphosphate synthesis and turnover that regulates the progression of endosomal transport. Novel Sac phosphatase joins the ArPIKfyve-PIKfyve complex. *J Biol Chem*. 2007;282(33):23878-23891. <http://doi.org/10.1074/jbc.M611678200>
4. Strunk BS, Steinfeld N, Lee S, et al. Roles for a lipid phosphatase in the activation of its opposing lipid kinase. *Mol Biol Cell*. 2020;31(17):1835-1845. <http://doi.org/10.1091/mbc.E18-09-0556>
5. Stutterd C, Diakumis P, Bahlo M, et al. Neuropathology of childhood-onset basal ganglia degeneration caused by mutation of VAC14. *Ann Clin Transl Neurol*. 2017;4(12):859-864. <http://doi.org/10.1002/acn3.487>
6. Wilson ZN, Scott AL, Dowell RD, Odorizzi G. PI(3,5)P₂ controls vacuole potassium transport to support cellular osmoregulation. *Mol Biol Cell*. 2018;29(13):1718-1731. <http://doi.org/10.1091/mbc.E18-01-0015>
7. Schulze U, Vollenbröker B, Braun DA, et al. The Vac14-interaction network is linked to regulators of the endolysosomal and autophagic pathway. *Mol Cell Proteomics*. 2014;13(6):1397-1411. <http://doi.org/10.1074/mcp.M113.034108>
8. Shisheva A, Sbrissa D, Hu B, Li J. Severe consequences of SAC3/FIG4 phosphatase deficiency to phosphoinositides in patients with Charcot-Marie-Tooth disease Type-4J. *Mol Neurobiol*. 2019;56(12):8656-8667. <http://doi.org/10.1007/s12035-019-01693-8>
9. Campeau PM, Lenk GM, Lu JT, et al. Yunis-Varon syndrome is caused by mutations in FIG4, encoding a phosphoinositide phosphatase. *Am J Hum Genet*. 2013;92(5):781-791. <http://doi.org/10.1016/j.ajhg.2013.03.020>
10. Lenk GM, Berry IR, Stutterd CA, et al. Cerebral hypomyelination associated with biallelic variants of FIG4. *Hum Mutat*. 2019;40(5):619-630. <http://doi.org/10.1002/humu.23720>
11. Lenk GM, Ferguson CJ, Chow CY, et al. Pathogenic mechanism of the FIG4 mutation responsible for Charcot-Marie-Tooth disease CMT4J. *PLoS Genet*. 2011;7(6):e1002104. <http://doi.org/10.1371/journal.pgen.1002104>
12. Lenk GM, Szymanska K, Debska-Vielhaber G, et al. Biallelic mutations of VAC14 in pediatric-onset neurological disease. *Am J Hum Genet*. 2016;99(1):188-194. <http://doi.org/10.1016/j.ajhg.2016.05.008>

13. Lines MA, Ito Y, Kernohan KD, et al. Yunis-Varón syndrome caused by biallelic VAC14 mutations. *Eur J Hum Genet.* 2017;25(9):1049-1054. <http://doi.org/10.1038/ejhg.2017.99>
14. Zhang Y, Zolov SN, Chow CY, et al. Loss of Vac14, a regulator of the signaling lipid phosphatidylinositol 3,5-bisphosphate, results in neurodegeneration in mice. *Proc Natl Acad Sci U S A.* 2007;104(44):17518-17523. <http://doi.org/10.1073/pnas.0702275104>
15. Mironova YA, Lenk GM, Lin JP, et al. PI(3,5)P2 biosynthesis regulates oligodendrocyte differentiation by intrinsic and extrinsic mechanisms. *Elife.* 2016;5:e13023. <http://doi.org/10.7554/eLife.13023>
16. Siddique AW, Ahmed Z, Haider A, Khalid H, Karim T. Yunis-Varon syndrome. *J Ayub Med Coll Abbottabad.* 2019;31(2):290-292.
17. Lenk GM, Frei CM, Miller AC, et al. Rescue of neurodegeneration in the Fig4 null mouse by a catalytically inactive FIG4 transgene. *Hum Mol Genet.* 2016;25(2):340-347. <http://doi.org/10.1093/hmg/ddv480>
18. Yunis E, Varón H. Cleidocranial dysostosis, severe micrognathism, bilateral absence of thumbs and first metatarsal bone, and distal apha-langia: a new genetic syndrome. *Am J Dis Child.* 1980;134(7):649-653. <http://doi.org/10.1001/archpedi.1980.02130190017005>
19. Baulac S, Lenk GM, Dufresnois B, et al. Role of the phosphoinositide phosphatase FIG4 gene in familial epilepsy with polymicrogyria. *Neurology.* 2014;82(12):1068-1075. <http://doi.org/10.1212/WNL.0000000000000241>
20. Kaur P, Bhavani GS, Raj A, Girisha KM, Shukla A. Homozygous variant, p.(Arg643Trp) in VAC14 causes striatonigral degeneration: report of a novel variant and review of VAC14-related disorders. *J Hum Genet.* 2019;64(12):1237-1242. <http://doi.org/10.1038/s10038-019-0678-1>
21. Liao S, Chen T, Dai Y, Wang Y, Wu F, Zhong M. Novel VAC14 variants identified in two Chinese siblings with childhood-onset striatonigral degeneration. *Mol Genet Genomic Med.* 2020;8(2):e1101. <http://doi.org/10.1002/mgg3.1101>
22. Lyon GJ, Marchi E, Ekstein J, et al. VAC14 syndrome in two siblings with retinitis pigmentosa and neurodegeneration with brain iron accumulation. *Cold Spring Harb Mol Case Stud.* 2019;5(6):a003715. <http://doi.org/10.1101/mcs.a003715>
23. Taghavi S, Chaouni R, Tafakhori A, et al. A clinical and molecular genetic study of 50 families with autosomal recessive parkinsonism revealed known and novel gene mutations. *Mol Neurobiol.* 2018;55(4):3477-3489. <http://doi.org/10.1007/s12035-017-0535-1>
24. Wright GC, Brown R, Grayton H, et al. Clinical and radiological characterization of novel FIG4-related combined system disease with neuropathy. *Clin Genet.* 2020;98(2):147-154. <http://doi.org/10.1111/cge.13771>
25. Sait H, Shambhavi A, Pandey M, Ravichandran D, Phadke SR. T2 olivary nuclei hyperintensities: a characteristic neuroimaging finding in FIG4-related leukoencephalopathy. *Am J Med Genet A.* 2023;191(3):864-869. <http://doi.org/10.1002/ajmg.a.63084>
26. Rajapurohitam V, Chalhoub N, Benachenhou N, Neff L, Baron R, Vacher J. The mouse osteopetrotic grey-lethal mutation induces a defect in osteoclast maturation/function. *Bone.* 2001;28(5):513-523. [http://doi.org/10.1016/s8756-3282\(01\)00416-1](http://doi.org/10.1016/s8756-3282(01)00416-1)
27. Chappard D, Palle S, Alexandre C, Vico L, Riffat G. Bone embedding in pure methyl methacrylate at low temperature preserves enzyme activities. *Acta Histochem.* 1987;81(2):183-190. [http://doi.org/10.1016/S0065-1281\(87\)80012-0](http://doi.org/10.1016/S0065-1281(87)80012-0)
28. Parfitt AM, Dreznar MK, Glorieux FH, et al. Bone histomorphometry: standardization of nomenclature, symbols, and units. Report of the ASBMR Histomorphometry Nomenclature Committee. *J Bone Miner Res.* 1987;2(6):595-610. <http://doi.org/10.1002/jbmr.5650020617>
29. Ducy P, Amling M, Takeda S, et al. Leptin inhibits bone formation through a hypothalamic relay: a central control of bone mass. *Cell.* 2000;100(2):197-207. [http://doi.org/10.1016/s0092-8674\(00\)81558-5](http://doi.org/10.1016/s0092-8674(00)81558-5)
30. Nicholson G, Lenk GM, Reddel SW, et al. Distinctive genetic and clinical features of CMT4J: a severe neuropathy caused by mutations in the PI(3,5)P2 phosphatase FIG4. *Brain.* 2011;134(Pt 7):1959-1971. <http://doi.org/10.1093/brain/awr148>
31. Liu Y, Bankaitis VA. Phosphoinositide phosphatases in cell biology and disease. *Prog Lipid Res.* 2010;49(3):201-217. <http://doi.org/10.1016/j.plipres.2009.12.001>
32. Karczewski KJ, Francioli LC, Tiao G, et al. The mutational constraint spectrum quantified from variation in 141,456 humans. *Nature.* 2020;581(7809):434-443. <http://doi.org/10.1038/s41586-020-2308-7>
33. Nakajima J, Okamoto N, Shiraiishi J, et al. Novel FIG4 mutations in Yunis-Varon syndrome. *J Hum Genet.* 2013;58(12):822-824. <http://doi.org/10.1038/jhg.2013.104>
34. Adès LC, Morris LL, Richardson M, Pearson C, Haan EA. Congenital heart malformation in Yunis-Varon syndrome. *J Med Genet.* 1993;30(9):788-792. <http://doi.org/10.1136/jmg.30.9.788>
35. Basel-Vanagaite L, Kornreich L, Schiller O, Yacobovich J, Merlob P. Yunis-Varon syndrome: further delineation of the phenotype. *Am J Med Genet A.* 2008;146A(4):532-537. <http://doi.org/10.1002/ajmg.a.32135>
36. Corona-Rivera JR, Romo-Huerta CO, López-Marure E, Ramos FJ, Estrada-Padilla SA, Zepeda-Romero LC. New ocular findings in two sisters with Yunis-Varón syndrome and literature review. *Eur J Med Genet.* 2011;54(1):76-81. <http://doi.org/10.1016/j.ejmg.2010.09.013>
37. Dworzak F, Mora M, Borroni C, et al. Generalized lysosomal storage in Yunis Varón syndrome. *Neuromuscul Disord.* 1995;5(5):423-428. [http://doi.org/10.1016/0960-8966\(94\)00089-r](http://doi.org/10.1016/0960-8966(94)00089-r)
38. Garrett C, Berry AC, Simpson RH, Hall CM. Yunis-Varon syndrome with severe osteodysplasty. *J Med Genet.* 1990;27(2):114-121. <http://doi.org/10.1136/jmg.27.2.114>
39. Hadipour Z, Shafeghati Y, Hadipour F. Yunis-Varón syndrome: the first report of two Iranian cases. *Acta Med Iran.* 2014;52(1):85-87.
40. Reutter H, Bagci S, Müller A, et al. Primary pulmonary hypertension, congenital heart defect, central nervous system malformations, hypo- and aplastic toes: another case of Yunis- Varón syndrome or report of a new entity. *Eur J Med Genet.* 2012;55(1):27-31. <http://doi.org/10.1016/j.ejmg.2011.09.002>
41. Umair M, Alkharfy TM, Sajjad S, Alfadhel M. FIG4-Associated Yunis-Varon syndrome: identification of a novel missense variant. *Mol Syndromol.* 2021;12(6):386-392. <http://doi.org/10.1159/000516971>